SEISMIC INTERACTION AMONG ON-GROUND AND UNDERGROUND STRUCTURES

J.M. Mayoral[(1)] and G. Mosqueda[(2)]

[(1)] Researcher, Institute of Engineering of the National University Autonomous of Mexico, jmayoralv@iingen.unam.mx
[(2)] Researcher, University of California at San Diego

Abstract

Seismic performance of buildings located in urban areas can be significantly affected by its interaction with underground structures. To date however, there is still a lack of proper understanding regarding the interplay between incoming seismic waves reflected in underground structures, and the energy feeding back from surface structures swinging back and forth during a large earthquake. In particular, due to its complexity, the effect that underground facilities, such as metro stations, tunnels and open shafts, have in the seismic response of strategic urban infrastructure such as buildings, urban overpasses, and medium to tall buildings is often ignored or its assessment is over simplified in practice. This, in turn, can lead to unsafe or costly designs. The results presented in this paper are part of and exhaustive numerical study aimed at assessing the ground motion variability associated to underground structures and its effects on strategic urban assets, such as tunnels and buildings, establishing detrimental or beneficial soil-structure interaction effects. Series of three-dimensional finite difference models were developed to study the proximity effect of the tunnel to the building, in the computed structural response. The building was assumed to be located in the highly compressible clay, found in Mexico City. From the results gathered in here, it was clearly stablished the ground motion modification in the surrounding soil that occur in the transversal ground motion component due to tunnel-building interaction.

Keywords: tunnel-building systems, soil-structure interaction, seismic response, resilience

1. Introduction

Public transportation networks in urban areas heavily rely on Transit Transfer Stations, TTS, to ensure a dependable and efficient connectivity. TTS are essential elements in transit networks of highly populated cities and airports [1], which facilitate travel connections among several public transportation systems, such as air and train routes, underground and bus transportation, and vehicles, contributing to urban integration and social equity [2]. TTS, are mostly comprised by sets of interconnected tunnel-building-bridges systems. Tunnel-building and tunnel-bridge interaction is potentially a major source of ground motion variability in the surrounding soil in urban areas, depending on soil conditions, tunnel cover, relative soil-tunnel stiffness, and non-linear effects at the tunnel-soil interface, which can lead to unsafe or costly design of the structures located nearby. To date however, there is a lack of technical data regarding the expected seismic performance of tunnel-building and tunnel bridges systems. This paper presents a numerical study of the seismic response of typical tunnel-building systems in soft clay, aiming at establishing detrimental or beneficial soil-structure interaction effects, considering several earthquake scenarios, defined through uniform hazard spectra. The results presented herein are part of a larger study, which involves both numerical modelling and instrumentation, conducted to assess the effect of the interaction among on-ground and underground structures in the seismic response of strategic infrastructure, for both normal and subduction events. Series of three-dimensional finite difference models were developed to study the proximity effect, in the computed structural response. The structures where assumed to be located in the highly compressible clay, found in Mexico City. Both normal and subduction events were considered. From the results gathered, it was clearly stablished the free field ground motion modification in the surrounding soil, which occur in the transversal ground motion componente due to tunnel-building interaction.

2. Idealized problem

Tunnel-building interaction in soft clay was studied considering the topology depicted schematically in Fig. 1, using a tridimensional finite difference model developed with the program FLAC^{3D}. The tunnel width, D, building high, H, and length, L, were assumed to be 11 m, 20 m and 20 m respectively, which corresponds to typical tunnel building typologies found in Mexico City. The distance between the tunnel and the building varied from 0 to 3 times the tunnel width, D, considering four cases as compiled in Table 1. The depth of the tunnel was keep constant and equal to two times the tunnel width (i.e. 22 m).

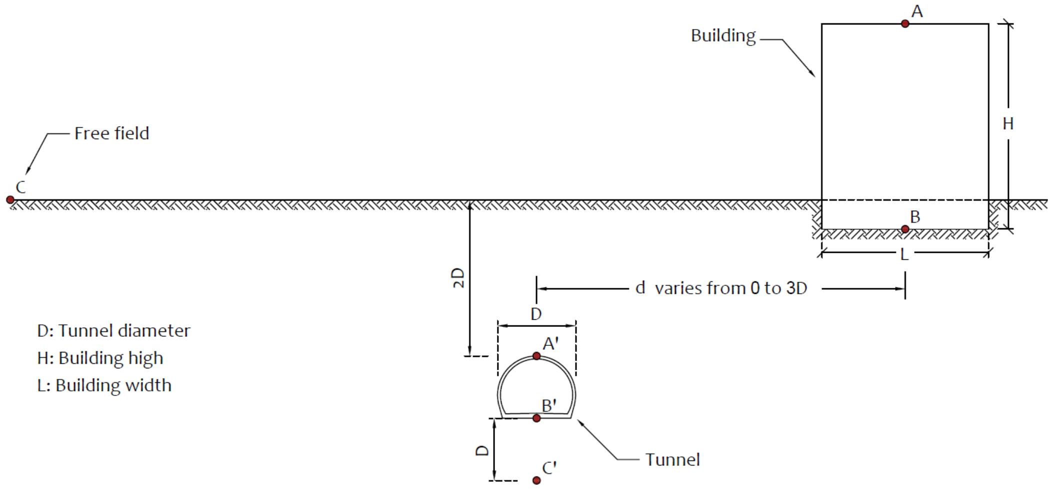

Fig. 1 – Schematic for the control points

Table 1 – Models considered and distances building/tunnel

Case	Distance between the tunnel, and the building (Diameters)
A	0
B	1
C	2
D	3

3. Soil profile

Fig. 2 shows the location of the site considered, which corresponds to an area in Mexico City where high plasticity clay is found. Typically, the soil profile in this area exhibits a desiccated crust of clay at the top, extending down to a depth of 1.0 m, which is underlain by a soft clay layer approximately 30.0 m thick, with interbedded lenses of sandy silts and silty sands. Underlying the clay there is a 5.0 m thick layer, in average, of very dense sandy silt, which rests on top of a stiff clay layer which goes up to a 60.0 m of depth (Fig. 3). Underneath this elevation a competent layer of very dense sandy silt is found.

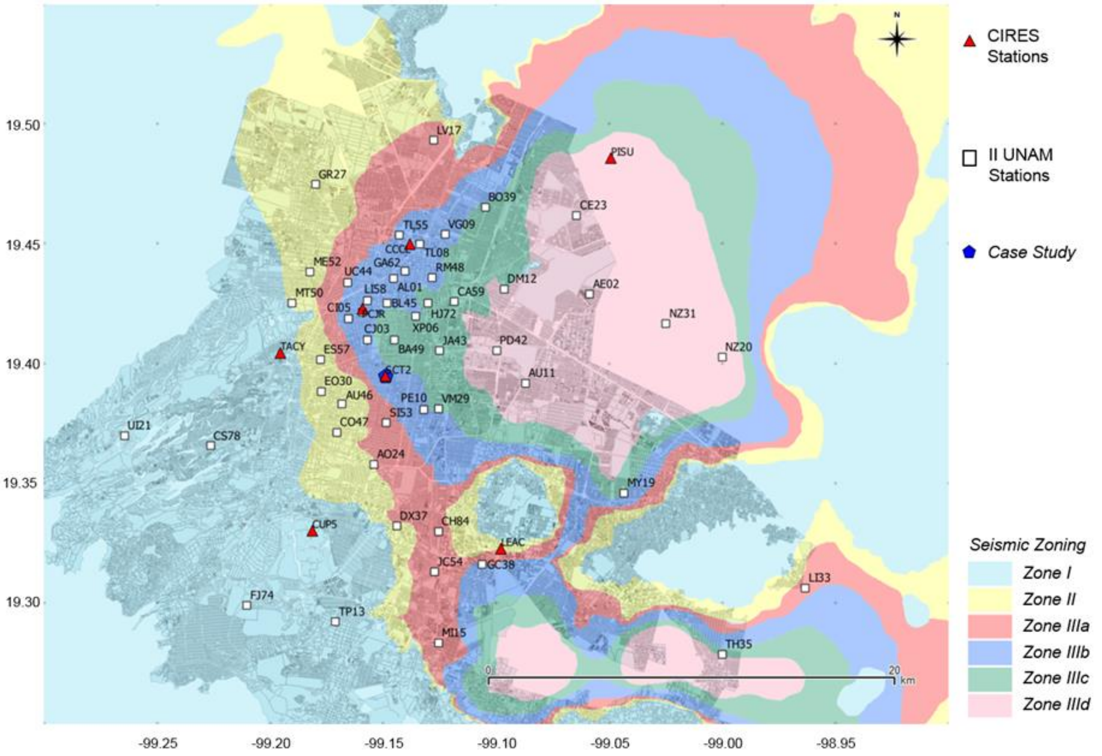

Fig. 2 – Map of subway lines and seismological stations in the city of Mexico

4. Dynamic properties

This site corresponds to the benchmark analyzed in the past by Seed and his coworkers [3], and corresponds to Zone IIIb. The shear wave velocity distribution was obtained using down-hole and P-S suspension logging technique [3], and is adjacent to the SCT seismological station. González and Romo´s model [4] was used to estimate the normalized modulus degradation and damping curves for clays (Fig. 4). For sands, the upper and lower bounds proposed by [5] for normalized modulus degradation and damping curves, respectively, were deemed appropriated. These curves had been used successfully in 1-D wave propagation analyses [3] to predict the measured response during the 1985 Michoacán earthquake.

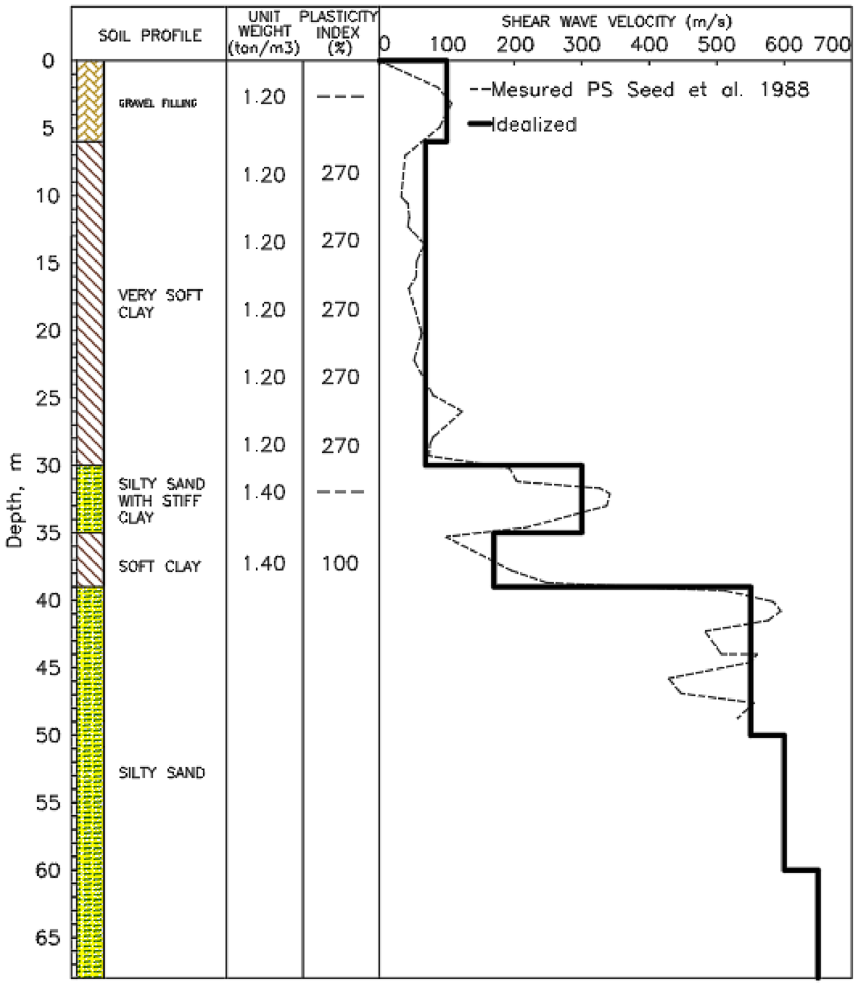

Fig. 3 – Soil profiles for study site

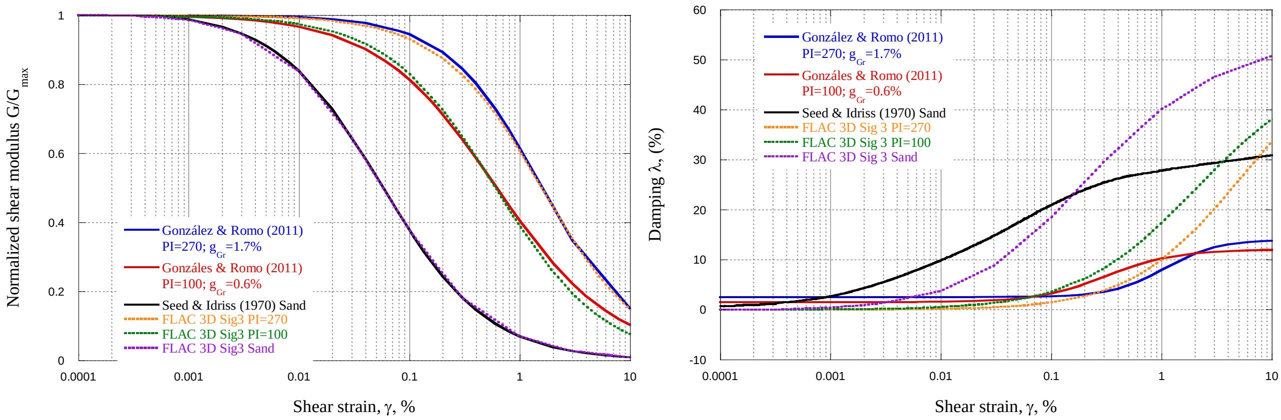

(a) (b)

Fig. 4 – Curves of (a) degradation of normalized shear stiffness, G/Gmax and (b) damping, λ

5. Building characteristics

A seven story 20 by 20 m^2 square footprint building, with a box-like foundation was considered in the parametric study. This building configuration exhibited the largest damage during the 2017 Mexico City earthquake [6]. Series of three-dimensional finite difference models were developed with the program FLAC^{3D} to simulate the seismic tunnel-soil-building interaction. The structure was simplified as a shear beam comprised by solid elements, with equivalent stiffness, k_i, and mass, m_i, for each story i. The dimensions of the equivalent shear beam are the same as those of the building considered. The mass is evenly distributed on each floor, as well as the shear modulus, G. The shear modulus can be obtained approximately with the Eq. (1), proposed by [7]:

$$G = \frac{F}{\Delta}\frac{h}{A} = \frac{F}{A}\frac{h}{\Delta} = \tau\frac{1}{\gamma} = \frac{\tau}{\gamma} \quad (1)$$

Where:
F/Δ is floor stiffness
h is floor height
A is the foot print structure area
τ is the equivalent shear stress in the solid element
γ is the equivalent angular deformation in the solid element

Thus, the structural period can be estimated as:

$$Te = 4\sum\sqrt{\frac{m_i}{k_i}} \quad (2)$$

Where:
m_i is the mass of each floor
k_i is stiffness of each floor

Table 2. Properties of building considered in the analysis.

Stories	Basements Levels	Te estimated for stiff buildings Stories*0.1 (s)	Te estimated for flexible buildings Stories*0.2 (s)	Te calculated using expression 2 (s)	Height (m)
7	2	0.7	1.4	1.01	21.0

6. Tunnel description

The tunnel geometry is shown in Fig. 5a. It was projected with an external height of 8.6 m and external width of 11 m, and primary and secondary linings. The primary lining is 0.2 m thick, and it is comprised of shotcrete reinforced with steel fibers (Fig. 5b), and the secondary lining is 0.4 m thick, and made of reinforced concrete (Fig. 5c). The compression strength of the primary lining concrete at 28 days, f'c, is about 25 MPa and 30 MPa for the secondary lining.

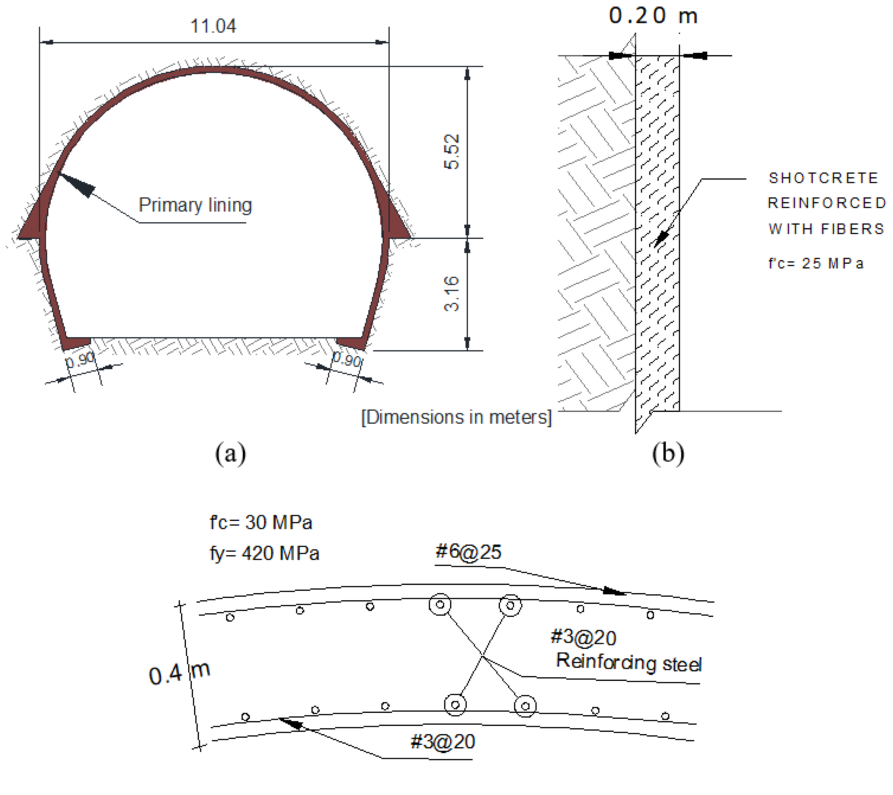

(c)

Fig. 5 – (a) Tunnel cross section, (b) primary lining, and (c) secondary lining

7. Seismic environment

The seismic environment was established through uniform hazard spectra developed for a return period of 250 years, as recommended in the Mexico City building code, considering normal events. The strong ground motion recorded during the September 19 2017 Puebla-Mexico earthquake at CU station, which is located at a rock outcrop, were used as input in the dynamic analyses. Fig. 6 shows the acceleration time history and the corresponding response spectra of the input ground motions. The characteristics of ground motion are described in Table 3.

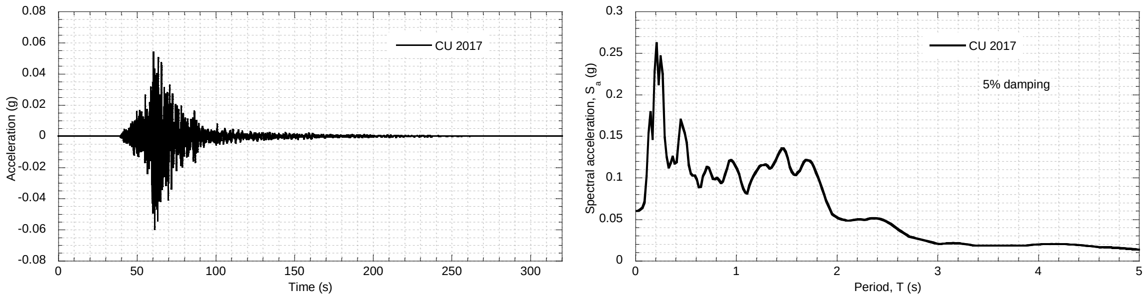

Fig. 6 – Accelerations time history and ground motion response spectra for normal event (CU 2017)

Table 3. Ground motion characteristic

Seismogenic zone	Earthquake name (Station)	Year	Moment magnitude Mw	PGA (g)	Duration (s)
Normal	Puebla-Mexico City (CU, Mexico)	2010	7.1	0.059	412

8. Free Field Response

Three-dimensional finite difference models of the free field were developed with the program FLAC^{3D}[8] and validated for the site considered, as depicted in Fig. 7. The ground motions were deconvolved to the base of each model using the software SHAKE [9]. The finite differences model of the free field has a depth of about 68m, and a 100 m by 100 m square section. The free field boundaries implemented in FLAC^{3D} were used along of the model.

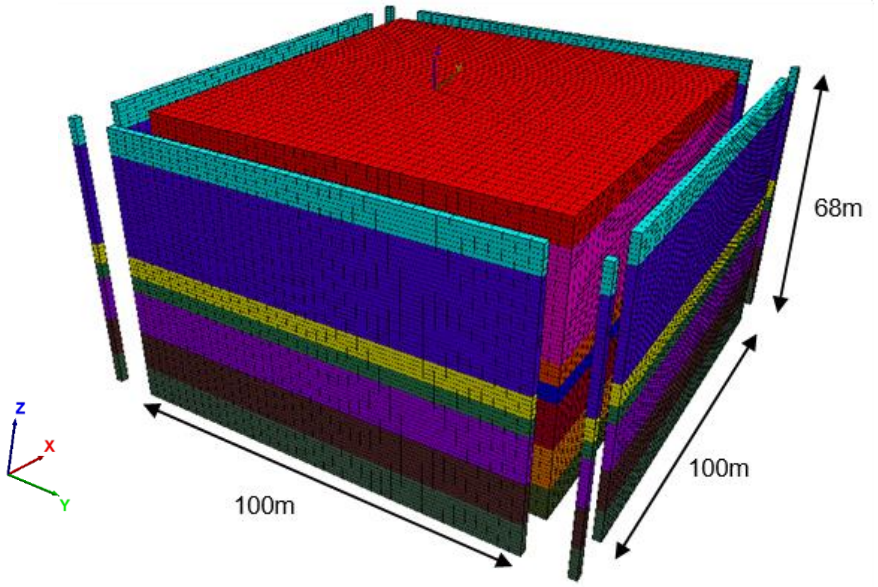

Fig. 7 – Three-dimensional finite difference soil column of studied site

A rigid base was considered along the bottom of the model to simulate the large dynamic impedance contrast existing at the site, in which a low shear wave velocity clay overlaid a high shear wave velocity bedrock. Soil nonlinearities were accounted for using equivalent linear properties, considering that the high plasticity Mexico City clay will exhibit a small amount of soil non-linearity for this level of shaking. The ground motion recorded at station CUP5 during the September 2017 earthquake, which is located at a rock outcrop, was used in the analysis. To establish the prediction capabilities of the model, the computed response was compared with the measured response at the site during the September 19, 2017 earthquake (Fig. 8). As can be noticed the predicted and measured response are in very good agreement.

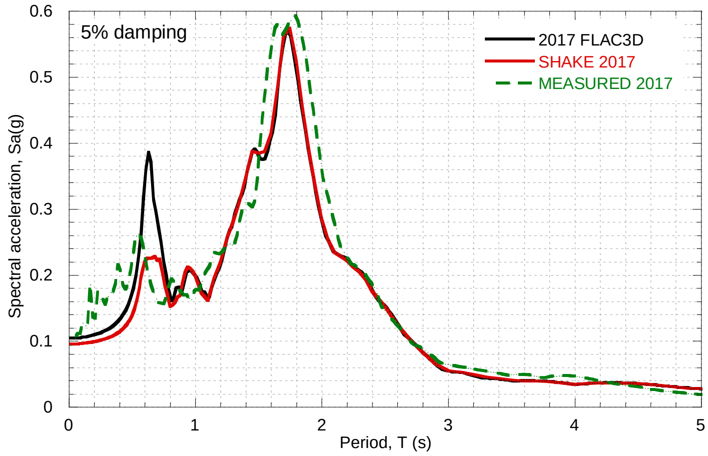

Fig. 8 – Response spectra calculated for the 2017 earthquake with FLAC^{3D}

9. Seismic tunnel-soil-structure interaction

Seismic underground structure-soil-surface structure interaction analyses were carried out with series of three dimensional finite difference models developed with the program FLAC^{3D}, considering different positions of the tunnel with respect to the building. Soil non-linearities associated to ground deformations are expected to occur, especially at the tunnel-soil and building-soil interfaces. Thus, a fully non-linear site response analysis was carried out using the program FLAC^{3D} [8]. The free field boundaries implemented in FLAC^{3D} were used along the edges of the model (Fig. 9). A flexible base was considered at the bottom of the model in the nonlinear analyses. Although several constitutive models have been developed to account for nonlinearities, to date, there is a lack of enough experimental data to develop and calibrate a high plasticity clay constitutive model. Thus, the practical oriented hysteretic model available in FLAC^{3D}, denominated as sig3 was used to approximately deal with both modulus stiffness degradation and damping variation during the seismic event. This model considers an ideal soil, in which the stress depends only on the deformation and not on the number of cycles. With these assumptions, an incremental constitutive relationship of the degradation curve can be described by $\tau_n/\gamma = G/G_{max}$, where τ_n is the normalized shear stress, γ is the shear strain and G/G_{max} the normalized secant modulus. The sig3 model is defined according to the Eq. (3):

$$\frac{G}{G_{max}} = \frac{a}{1+exp\left(-\frac{L-x_0}{b}\right)} \qquad (3)$$

where L is the logarithmic strain defined as L = log10(γ), and the parameters a, b, and x0, used by the sig3 model were obtained by an iterative approach, in which the modulus degradation curves were fitted with the model equations. The corresponding damping is given directly by the hysteresis loop during cyclic loading. For the cases studied herein, the parameters "a", "b", and x_o vary from 1 to 1.014, -0.46 to -0.55, and 0.2 to -1.5, respectively. Nonlinear soil behavior is a function of the shaking level, which, if high, leads to shear stiffness degradation and damping increase. The fact that FLAC^{3D} generates larger damping at high strains than experimentally-derived curves is due to the very well-known limitation of hysteretic-type models, which are not able to fully capture simultaneously both shear stiffness degradation and damping curves developed under steady state conditions. However, in a nonlinear analysis, it is attempted to characterize the transient ground response in each loading cycle as a function of the evolution of shear strains during ground shaking, rather than the steady state response established in the resonant column and cyclic triaxial test from which modulus degradation and damping curves, such as Seed and Idriss model were developed.

A Fig. 9 shows the numerical model for the cases analyzed. This figure also includes the control points considered.

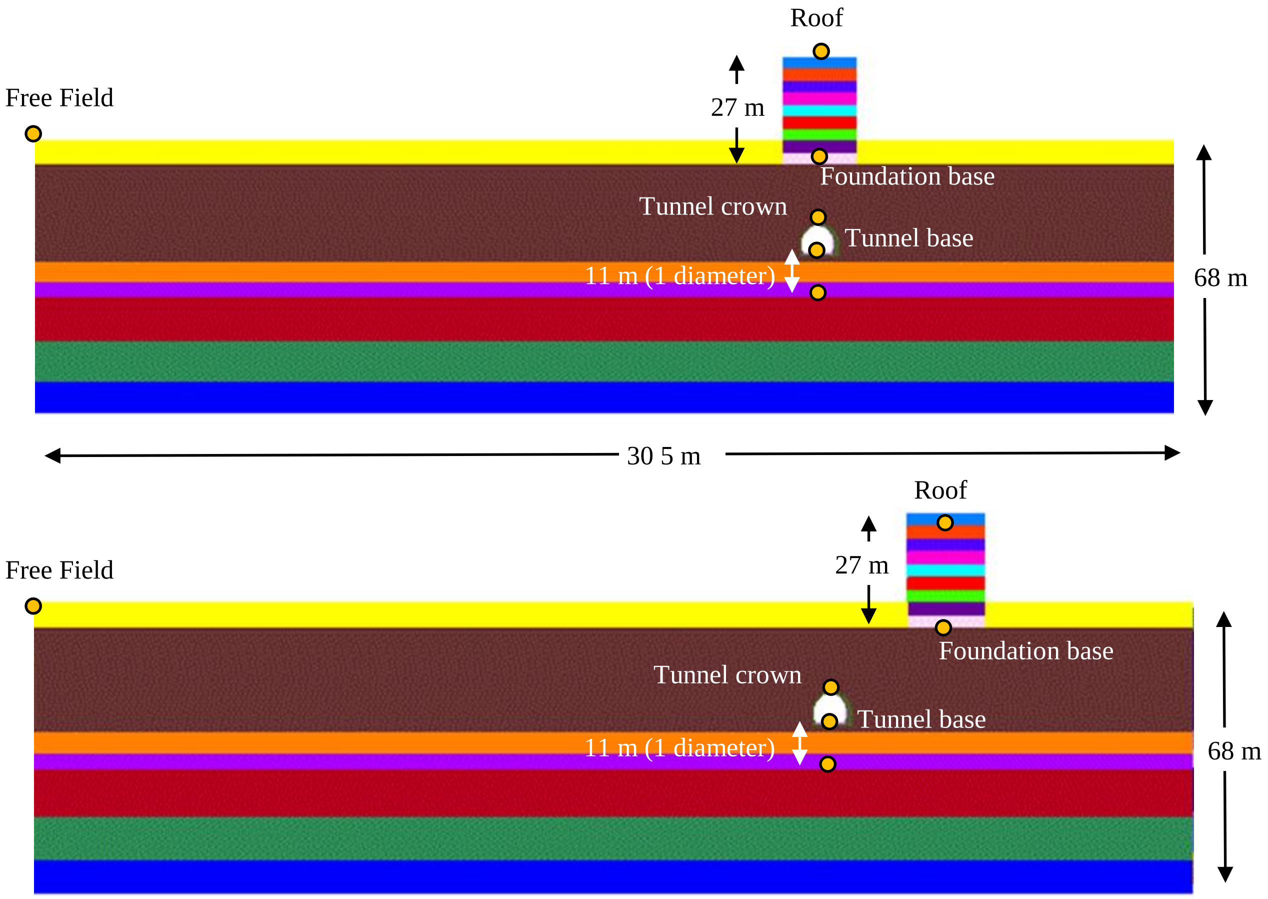

Fig. 9 – Three-dimensional finite difference models considering the tunnel underneath the building (a), and 3D away from the building (b)

10.Effect of the tunnel in the seismic response of the building

Fig. 10 shows the effect of the tunnel in the relative amplitude of the amplification factor, defined as the ratio of the spectral accelerations computed at the surface with respect to those computed at the base of the building, for both the transversal (i.e. across the tunnel section, x direction), and longitudinal directions (i.e. along the tunnel axis, y direction). As can be clearly noticed, the maximum detrimental tunnel-building interaction response in the transversal direction occurs when the tunnel is underneath the building. Thus, this factor goes from 4 to 7, when the distance between the tunnel and the building goes from 3D to zero, for a structural period of 1.8s. In this case, the amplification is larger for the normal event, due to the fact the predominant period of the excitation for normal events is closer to the fundamental period of the soil. This fact should be taken into account to proper estimate the seismic demand in the surrounding structures. On the other hand, this effect does not show in the longitudinal direction, in which the amplification factor seems to be independent of the tunnel location. Regarding the effect of the interaction between the building and tunnel in the distribution of vertical accelerations. Figs. 11 and 12 shows the response spectra computed at the tunnel crown, one diameter below the tunnel, and at surface. It is clearly seen the complex coupling between the seismic waves coming from the earthquakes and those associated to the diffraction with the tunnel and the energy feeding back from the structure.

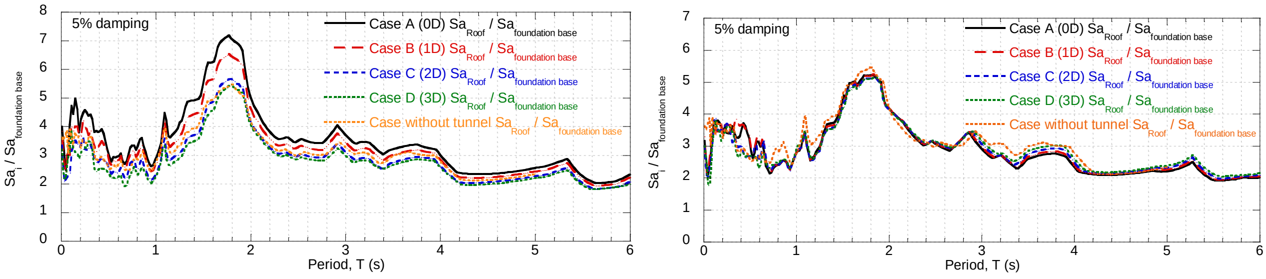

(a) (b)

Fig. 10 –Response spectra normalized with respect to foundation base at control points for the 2017 earthquake in a) X direction (transverse to the tunnel), and b) Y direction (longitudinal to the tunnel)

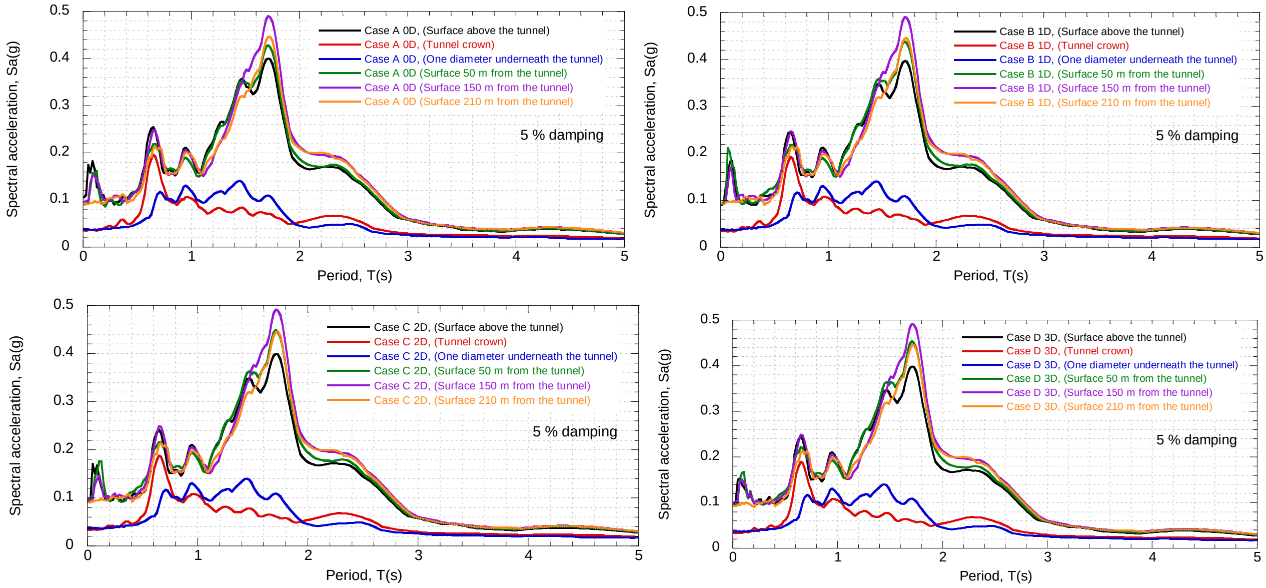

Fig. 11 – Response spectra for the 2017 earthquake in X direction (transverse to the tunnel)

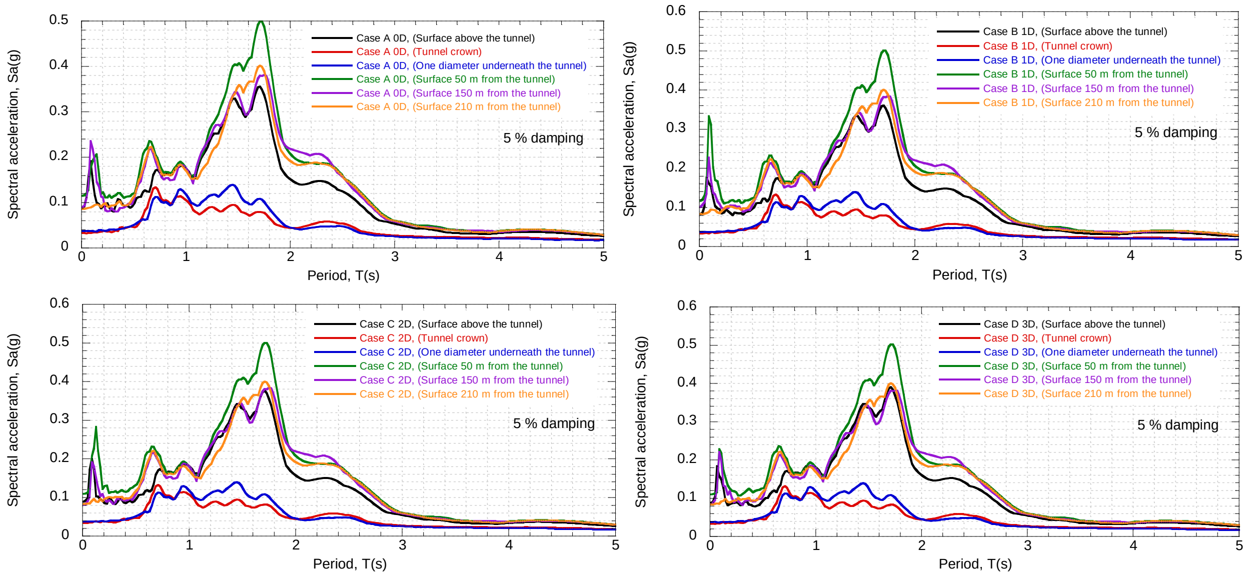

Fig. 12 –. Response spectra for the 2017 earthquake in Y direction (longitudinal to the tunnel)

Fig. 13 shows the variation of the PGA at the ground surface with respect to the distance from the tunnel for different locations of the tunnel. It is clearly seen that the relative location between the tunnel and the building impacts strongly the PGA distribution in the proximity of the building. For all the cases analyzed, the building tends to reduce the ground response due to the relative high stiffness of the foundation, in comparison with the stiffness of the surrounding soil (i.e. soft clay). This effect is more notorious in the longitudinal direction. The maximum PGA occurs for the case A, when the tunnel is underneath the building, and it goes up to 1.4, occurring at about 5 times diameter, and can occur at larger distances form the tunnel (i.e. 100m), due to the small amount of damping, and stiffness degradation expected to developed in the high plasticity clays found in Mexico City.

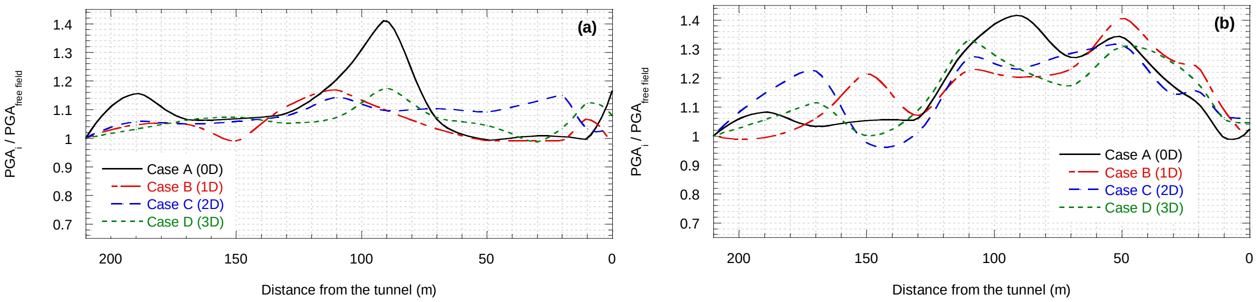

Fig. 13 –. Evolution of the PGA normalized with respect to PGA in free field for the 2017 earthquake in the a) X direction and b) Y direction

Regarding the potential effects in nearby buildings, Fig. 14 shows the spectral ratio (Sa_{max}/Sm_{axff}) distribution with distance measured from the building axis. Interestingly, an important amplification of the expected free field ground motions occurs, in the near field, at a distance ranging between 50 to 150 meters from the building. This fact should be taken into account when assessing the seismic performance of nearby structures, especially if there are light weight 1 to 4 story buildings.

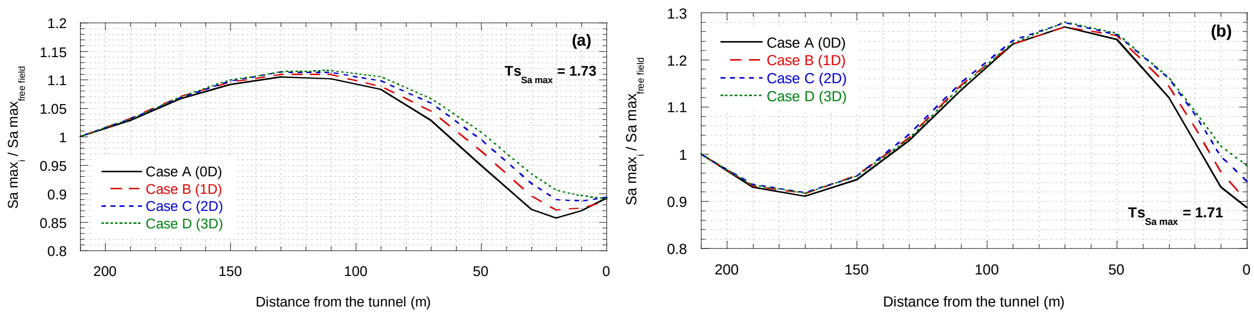

Fig. 14 –. Evolution of the Sa_{max} normalized with respect to Sa_{max} in free field for the 2017 earthquake in the a) Transverse direction and b) longitudinal direction

11.Conclusions

This paper presents part of and exhaustive numerical study aimed at assessing the ground motion variability associated to underground structures and its effects on strategic urban assets, such as tunnels and buildings, establishing detrimental or beneficial soil-structure interaction effects. Series of three-dimensional finite difference models were developed to study the proximity effect of the tunnel to the building, in the computed structural response. As can be clearly noticed, the maximum detrimental tunnel-building interaction response in the transversal direction occurs when the tunnel is underneath the building. Thus, this factor goes from 4 to 7 when the distance between the tunnel and the building goes from 3D to zero, for a structural period of 1.8s. The amplification is larger for the normal event, due to the fact the predominant period of the excitation for normal events is closer to the fundamental period of the soil. This fact should be taken into account to proper estimate the seismic demand in the surrounding structures. On the other hand, this effect does not show in the longitudinal direction, in which the amplification factor seems to be independent of the tunnel location. For all the cases analyzed, the building tends to reduce the ground response due to the relative high stiffness of the foundation, in comparison with the stiffness of the surrounding soil (i.e. soft clay). This effect is more notorious in the longitudinal direction. From the results gathered herein, it was clearly stablished the free field ground motion modification that occur in the transversal ground motion component due to tunnel-building interaction, in the surrounding soil, at distances ranging from 50 to 100m, due to the large linear range observed in Mexico City high plasticity clay. This fact should be taken into account when assessing the seismic performance of nearby structures, especially if there are light-weighted 1 to 4 story dwellings.

12. References

[1] Orth H, Weidmann U (2015). Quantifying the effects of activity concentration at airports on public transport using an iterative reduction procedure. Transportation Research Procedia 10: 503-513.

[2] Román A, Mayoral JM, Román L (2018). A novel approach for transit transfer stations design optimization in densely populated cities. Procedia Computer Science 130:1013-1018.

[3] Seed HB, Romo MP, Sun J, Jaime A, Lysmer J. (1988). Relationships between soil conditions and earthquake ground motions. J Earthq Spectra 1988;4(2):687–730.

[4] González CY, Romo MP. Estimation of clay dynamic properties. Rev Ing Sísmica 2011;84:1–23.

[5] Seed HB, Idriss IM. Soil moduli and damping factors for dynamic response analysis. (UCB/EERC-70/10).

[6] Mayoral JM, Tepalcapa S, Roman A, Mohtar CS, Rivas R, (2019). Ground Subsidence and its implication on building seismic performance. Soil Dynamics and Earthquake Engineering, Volume 126, November 2019, 105766

[7] Romo MP, Barcena A. (1994). Dynamic soil-structure interaction of Mexico City (In Spanish). UNAM series 565

[8] Itasca Consulting Group. FLAC3D, Fast Lagrangian Analysis of Continua in 3 Dimensions, User's Guide

[9] Schnabel PB, Lysmer J, Seed HB. SHAKE: A Computer Program for Earthquake Responser Analysis of Horizontally Layered Sites. CA: College of Engineering, Report No. EERC 72-12, University of Berkeley; 1972

